

## Experimental Studies of Electric Currents in the Divertor Plasma of a Helical Device

CHECHKIN Viktor\*, VOITSENYA Vladimir, SMIRNOVA Marina, SOROKOVOJ Eduard, MIZUUCHI Tohru<sup>1</sup>, NAGASAKI Kazunobu<sup>1</sup>, OKADA Hiroyuki<sup>1</sup>, HAYAKAWA Aturo<sup>1</sup>, HAMADA Takateru<sup>1</sup>, SANO Fumimichi<sup>1</sup>, OBIKI Tokuhiko<sup>1</sup>, ZUSHI Hideki<sup>2</sup>, NAKASUGA Masahiko<sup>3</sup>, BESSHO Sakae<sup>3</sup>, KONDO Katsumi<sup>3</sup>, FUNABA Hisamichi<sup>4</sup>, MASUZAKI Suguru<sup>4</sup> and MOTOJIMA Osamu<sup>4</sup>

*Institute of Plasma Physics, National Science Center*

*“Kharkov Institute of Physics and Technology”, Kharkov 310108, Ukraine*

*<sup>1</sup>Institute of Advanced Energy, Kyoto University, Gokasho, Uji 611-0011, Japan*

*<sup>2</sup>Research Institute for Applied Mechanics, Kyushu University, Kasuga 816-0811, Japan*

*<sup>3</sup>Graduate School of Energy Science, Kyoto University, Gokasho, Uji 611-0011, Japan*

*<sup>4</sup>National Institute for Fusion Science, Toki 509-5292, Japan.*

(Received: 18 January 2000 / Accepted: 23 May 2000)

### Abstract

In the  $l = 2/m = 19$  Heliotron E device, with currentless NBI and NBI+ECH plasmas, measurements were made of electric currents flowing to grounded collector plates installed near the vacuum chamber wall in 4 poloidal cross-sections of the torus within  $1/2$  helical pitch. A strong up-down asymmetry in both absolute value and sign was observed in the currents flowing along the diverted field lines. In general case, the value and direction of the current depended on absorbed power. Proceeding from the character of current response to fast variations of the heating power, it was hypothesized that non-ambipolar divertor flows were strongly affected by dynamics of suprathreshold particles occurring in the plasma during NBI and ECH.

### Keywords:

heliotron, divertor, non-umbipolar flow, up-down asymmetry, helical ripple asymmetry, fast particles

### 1. Introduction

Diverted field lines are a natural component of a heliotron/torsatron magnetic configuration. Since a potential difference is always present between the edge plasma and the wall, an electric current arises along the diverted lines, its value and direction depending on poloidal/toroidal distribution of the edge potential, which in turn is affected by processes developing in the SOL and core plasmas. The understanding of the physical nature of this current (further on, ‘plasma current’,  $I_p$ ) as an intrinsic part of the mechanism of particle and heat loss is of primary importance for a

realistic design of any divertor facility and the regime of its operation.

Earlier, measurements of floating potential  $V_f$  and current  $I_p$  near the chamber wall in the Heliotron E device under ECH and NBI conditions [1,2] evidenced non-ambipolarity of the plasma flows coming to the wall. The purpose of this work made on Heliotron E with NBI and NBI+ECH plasmas is (1) to elucidate the poloidal/toroidal structure of non-umbipolar divertor flows near the wall; (2) to find the relationship between  $I_p$  and heating power for most intense diverted plasma

\*Corresponding author's e-mail: [checkkin@ipp.kharkov.ua](mailto:checkkin@ipp.kharkov.ua)

flows ('main divertor flows', MDFs); (3) to discuss some possible mechanisms of non-ambipolar divertor flow drive in a helical device.

**2. Experimental Conditions**

The Heliotron E device [3] is an  $l = 2/m = 19$  heliotron,  $R_o = 2.2$  m,  $\bar{a} \approx 0.2$  m. The whole edge structure of the magnetic field with 'X-points' was well inside the chamber. The toroidal magnetic field was fixed at  $B_\phi = 1.9$  T, with  $\approx 2$  cm inward shift of the magnetic axis ( $\beta^* = -0.192$ ). The rotational transform was  $t(\bar{a})/2\pi \approx 2.8$ .

Currentless plasmas were produced by fundamental ECH ('ECH-1', 53.2 GHz,  $\leq 0.4$  MW) or 2nd harmonic ECH ('ECH-2', 106.4 GHz, 0.3 MW), then they were supported and heated by NBI (injection voltage 23–24 keV, injected power  $P_{inj} \leq 3$  MW, injection angles  $62^\circ$ ,  $79^\circ$ ,  $90^\circ$ , pulse length up to 160 ms). A 30 ms ECH pulse was imposed on NBI in some cases ("NBI+ECH"). Typical plasma parameters were  $\bar{n}_e \approx (1.5\text{--}2.5) \times 10^{19} \text{ m}^{-3}$ ,  $T_e(0) \approx 0.6\text{--}1.5$  keV,  $T_i(0) \approx 0.3\text{--}0.6$  keV.

To detect plasma currents, 56 collected plates (CPs,  $(5.0 \times 0.8) \text{ cm}^2$ ) were used [1]. 7-plate arrays were arranged poloidally close to the wall on both rounded parts of the vacuum chamber in 4 poloidal cross-sections with the interval of  $1/8$  field period (Fig. 1). The position of each array was defined by the poloidal angle  $\Theta$  of its center:  $\Theta = 0^\circ, 45^\circ, 90^\circ, 135^\circ, 180^\circ, 225^\circ, 270^\circ, 315^\circ$ .

In Fig. 2 calculated plots of connection length  $L$  against poloidal angle  $\theta$  are drawn with solid lines for

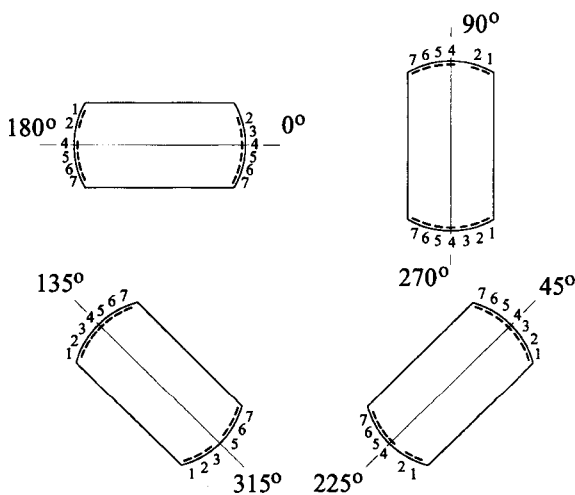


Fig. 1 Disposition of CP arrays.

open field lines, whose starting points lie on the lines of CP array disposition. The interval of calculation was  $\Delta\theta = 0.5^\circ$ . CP positions 1,2,...,7 in each array are marked by fat segments. The field lines starting in the  $B_\phi$  direction and against it form the families A and B, respectively. These data allowed one to find the plates to be expected to collect the MDFs A-0, B-0, A-45, B-45, etc. A helical vertical symmetry ('up-down symmetry') is inherent to the calculated  $L(\Theta, \theta)$  distributions, where each family A(B) in the top half of the torus corresponds to the family B(A) in the bottom half with symmetric  $\theta$ -distribution against the midplane.

**3. Spatial Distribution of Plasma Currents**

In Fig. 2 a shaded rectangle is attached to each CP, its height being proportional to the plasma current  $I_p$  (NBI,  $P_{inj} \approx 0.7$  MW,  $\bar{n}_e \approx 2 \times 10^{19} \text{ m}^{-3}$ ). Except plates 4 ( $\Theta = 90^\circ$ ) and 6 ( $\Theta = 270^\circ$ ), within each CP array the maxima of  $I_p$  fall at those of  $L$ , though, in general, there is no definite relationship between the values of  $I_p$  and  $L$ .

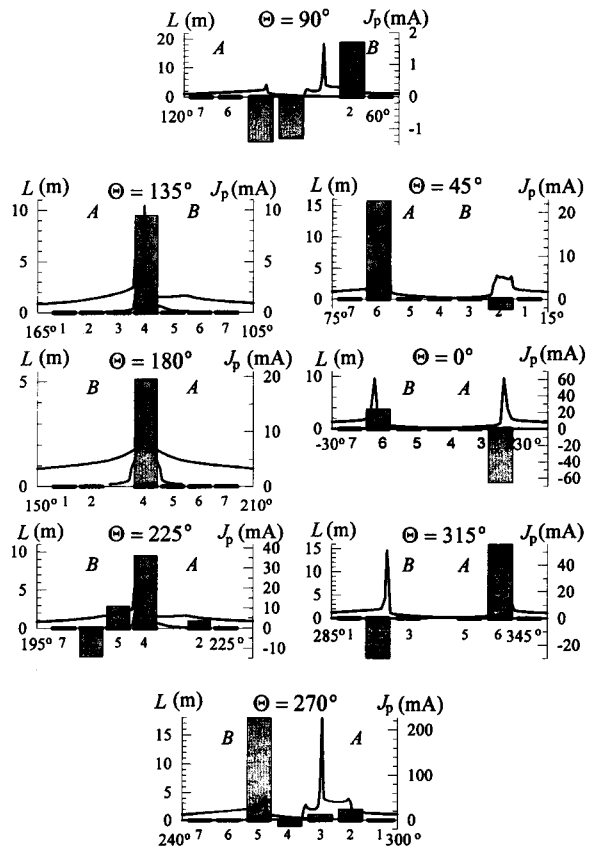


Fig. 2 Calculated connection length  $L$  versus poloidal angle (solid lines). Distribution of plasma current  $I_p$  in collector plates (shaded rectangles).

In contrast to  $L(\Theta, \theta)$  distributions, the measured  $I_p(\Theta, \theta)$  distributions were characterized by a strong vertical asymmetry, in particular, by (1) a multiple  $|I_p|$  increase when going from the top to the bottom, and (2) opposite  $I_p$  directions in the symmetrically positioned MDF pairs A-90/B-270, A-45/B-315, A-0/B-0, where calculated poloidal locations of starting points and ends of the field lines were clearly separated and lay on different sides of the midplane. In particular, opposite directions of  $I_p$  in the A-90/B-270 pair evidence an electron excess in the top part and an ion excess in the bottom part of the edge plasma to be formed under Fig. 2 conditions.

#### 4. Plasma Heating Effect on $I_p$

The  $I_p/(\bar{n}_e - P_{abs}/\bar{n}_e)$  plots,  $P_{abs}$  being a power absorbed in the plasma [4], are shown in Figs. 3 and 4 for two pairs of MDFs A-90/B-270 and A-0/B-0, as a way of example. In addition to the NBI-only heating (○, ●), the data for NBI+ECH-1(△, ▲) and NBI+ECH-1+ECH-2 (◇, ◆) are also presented. The spread of experimental points could be caused at least by a non-precised shot-to-shot reproducibility of plasma parameters, non-accurate measurements of  $I_p$  (especially, small  $I_p$ s specific for the top part), an approximate character of the relation for  $P_{abs}$  [4]. Though the interpolating straight lines are drawn through the NBI-only points, a similar dependence seems to take place for the combined heating too. In the A-90/B-270 pair on the top and bottom, respectively, the current  $I_p$  reversed in the interval of 200–300 kW/10<sup>19</sup>

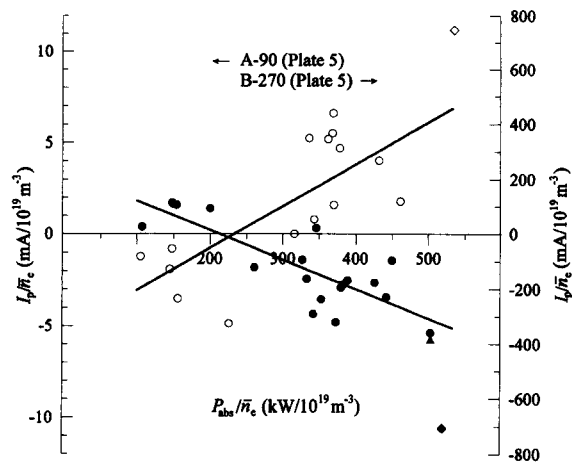


Fig. 3 Density-normalized plasma current versus density-normalized absorbed power for the MDFs A-90 (○, △, ◇) and B-270 (●, ▲, ◆).

m<sup>-3</sup> (Fig. 3). Thus, the regions with the excess of ions and electrons in the lower and upper parts of the torus, respectively, interchanged their positions. At the same time, it seems that the current  $I_p$  in the A-0/B-0 pair near the midplane (Fig. 4) either reversed at a much smaller  $P_{abs}/\bar{n}_e$  (<50 kW/10<sup>19</sup> m<sup>-3</sup>) or did not change the direction at all.

#### 5. $I_p$ Response to a Fast Variation of Heating Power

The  $I_p/\bar{n}_e - P_{abs}/\bar{n}_e$  dependencies shown in Figs. 3, 4 were measured 30 ms after start of injection, when the processes of edge plasma potential and corresponding plasma current formation presumably attained a (quasi) steady state. When shorter NBI (50 ms) or ECH (30 ms) pulses with steep leading and trailing edges ( $\leq 1$  ms) were imposed on a longer (160 ms) NBI, the  $V_f$  and  $I_p$  changes in MDFs generally underwent two phases, fast ( $\leq 1$  ms) and slow ones ( $\geq 10$  ms, the order of confinement time). The fast phase showed itself in a more or less steep bend of  $V_f$  and  $I_p$  time traces at the moments of additional heating switched on and off. As a way of example, in Fig. 5 time traces of  $V_f$  are shown in the MDFs B-270 and B-0 with additional NBI (a) and ECH (b). In the case (a), fast and slow  $V_f$  ( $I_p$ ) changes in a given MDF always had the same direction. In the case (b), the slow changes had the same direction as in the case (a), while the fast changes could be directed opposite to the slow ones in some MDFs, in particular, in B-0. This could evidence a different physical nature of fast and slow changes. The fast decay or rise of  $V_f$  and  $I_p$  after additional (or full) heating switched off

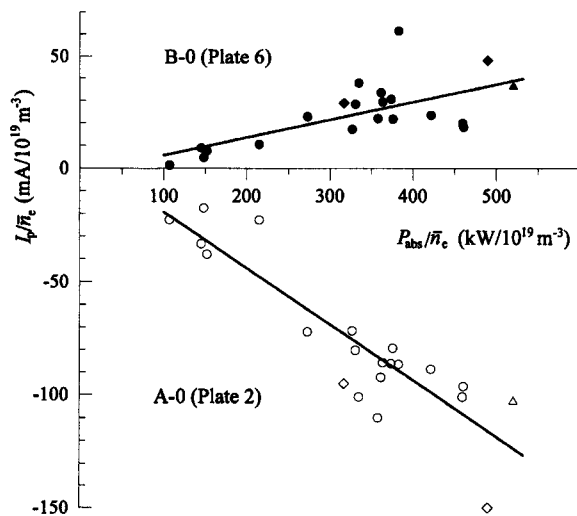


Fig. 4 Same as Fig. 3 for the MDFs A-0 and B-0.

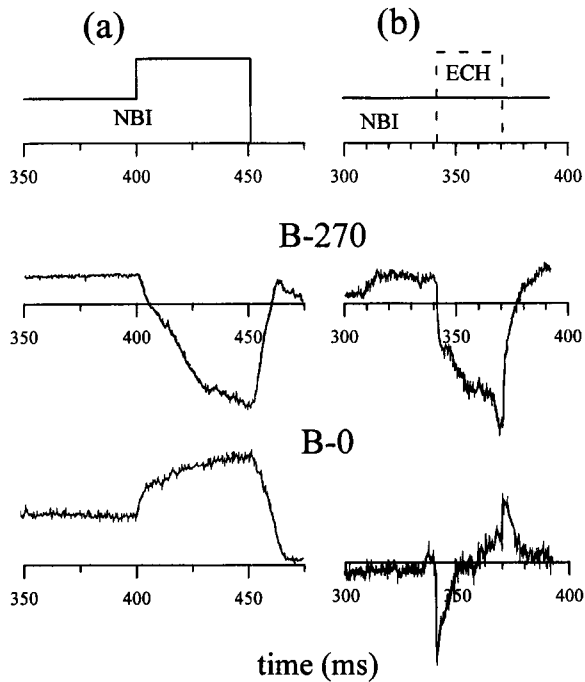


Fig. 5 Potential  $V_f$  response to an additional NBI (a) and ECH (b) pulse imposed on a long NBI.

means that the processes giving rise to the fast phase persisted under (quasi) stationary conditions.

## 6. Discussions

Among mechanisms giving rise to parallel electric currents in the diverted SOL plasma of a tokamak, the thermoelectric effect [5] is discussed, first of all. In the Heliotron E device under conditions considered, the electron temperature  $T_e$  near CPs in the MDFs, as estimated by measured values of  $V_f$ ,  $I_p$  and ion saturation current  $I_s$ , occurred obviously higher in the lower half of the torus irrespective of the value of  $P_{abs}/\bar{n}_e$ . Nevertheless, the direction of  $I_p$  in the A-90/B-270 pair (Figs. 2, 3) coincided with the expected direction of the thermoelectric current (from 'hot' to 'cold' side) only at a large power ( $P_{abs}/\bar{n}_e > 200 \text{ kW}/10^{19} \text{ m}^{-3}$ ), and it was opposite to the calculated parallel current direction in the SOL at a small power even with a non-zero parallel electron pressure gradient [6] taken into account. Therefore, it seems that the thermoelectric effect did not contribute seriously to the plasma currents in the Heliotron E case.

As another approach, a possible connection of non-ambipolar divertor flows with particle dynamics in the confinement volume is considered. A redistribution or predominant escape of ions (electrons) from certain

regions of confinement volume will give rise to selfconsistent changes of edge plasma potential and to corresponding electric currents along open field lines. The fast changes of  $V_f$  and of  $I_p$ , consequently, with an additional heating switched on and off (Fig. 5) could result from convective motions of suprathermal electrons and ions, while slow  $V_f$  and  $I_p$  variations were caused by diffusion-like processes with participation of thermal particles.

It follows from Figs. 2, 3 that at a small heating power excesses of electrons and ions occurred at the top and bottom of the confinement region, respectively. With a heating power increase, the electron and ion regions reversed, the process of reversing to be of convective character (Fig. 5). A strong up-down asymmetry remained after this transition. As was shown in [4], the asymmetry existed even in the limit of zero power. It was supposed that this 'initial' asymmetry resulted from distortions of the real magnetic structure of the divertor layer (by analogy with double-null divertor in a tokamak [7]). With NBI or ECH application, a further modification, enhancement of the asymmetry could result from a redistribution and escape of some groups of fast particles due to the effect of vertical asymmetry of the helical field ripple [8]. For some magnetic configurations, including that of Heliotron E, such asymmetry is a natural one [9]. On the basis of theory [9-13] and experimental data from the Heliotron E and CHS helical devices [14], the following qualitative power-governed scenario of convective motions of fast particles in Heliotron E can be hypothesized.

At a low  $P_{abs}$ , when the ambipolar electric field  $E_r$  is small ( $\Omega_{\nabla B} \gg \Omega_{E \times B}$ ,  $\Omega_{\nabla B}$  and  $\Omega_{E \times B}$  are the frequencies of poloidal precession due to  $\nabla B$  drift and of poloidal rotation, respectively) and negative ('ion root'), the character of loss cone losses is not strongly affected by  $E_r$ . In this case, most of fast escaped particles are toroidal banana-ions transformed into helical bananas at the periphery. Owing to the vertical asymmetry of the helical ripple wells, these particles undergo a vertical drift downwards, just where a maximum positive current  $I_p$  was observed (Figs. 2, 3). The toroidal banana-electrons with transient orbits drift upwards, resulting in a small negative current  $I_p$ .

With  $P_{abs}$  increase accompanied by  $E_r$  increase, the helical resonance  $\Omega_{\nabla B} + \Omega_{E \times B} \approx 0$  [12] for fast ions can occur ( $E_r \sim -100 \text{ V/cm}$  for Heliotron E). Since a large fraction of these particles is transformed into superbananas and drifts upwards, the vertical asymmetry

of non-ambipolar divertor flows can be in part or completely compensated.

With a further  $P_{abs}$  increase and an accompanying  $T_e$  increase, another specific case may arise after a fast transition from  $E_r < 0$  to  $E_r > 0$  [14] ('electron root'). Here, the majority of fast ions are well confined deeply trapped ones, and a loss of fast superbanana-electrons dominates. The latter drift downwards, where a large negative current  $I_p$  was observed at large  $P_{abs}/\bar{n}_e$  (Fig. 3). Only a small fraction of fast ions is transformed into superbananas in this state and drifts upward.

An obvious merit of this hypothesis is in combination of both most remarkable features of non-ambipolar divertor flows in Heliotron E, their strong up-down asymmetry and the reverse with heating power.

### Acknowledgements

The authors are grateful to all members of the Heliotron Group for their support and collaboration and to Dr. K. Hanatani for very helpful discussions.

This work was partly supported by the collaboration program of the Laboratory for Complex Energy Processes, IAE, Kyoto University, and by the Fundamental Studies Foundation of the Ministry of Science and Technologies of Ukraine.

### References

- [1] T. Mizuuchi *et al.*, in *Controlled Fusion and Plasma Physics (Proc. 18th Eur. Conf. Berlin, 1991)*, Vol. 15B, Part III (EPS, Geneva, 1991), p. III-65.
- [2] V.V. Chechkin *et al.*, in *Controlled Fusion and Plasma Physics (Proc. 24 EPS Conf., Berchtesgaden, 1997)*, Vol. 21A, Part IV (Geneva, 1997), p. 0901.
- [3] T. Obiki *et al.*, *Fusion Technol.* **17**, 101 (1990).
- [4] V.V. Chechkin *et al.*, *Nucl. Fusion* **40**, 785 (2000).
- [5] P.J. Harbour, *Contrib. Plasma Phys.* **28**, 417 (1988).
- [6] J.M. Staebler and F.L. Hinton, *Nucl. Fusion* **29**, 1820 (1989).
- [7] R. Marchand *et al.*, *Nucl. Fusion* **35**, 297 (1995).
- [8] P.N. Yushmanov *et al.*, *Nucl. Fusion* **33**, 1293 (1993).
- [9] M.S. Smirnova, *Phys. Plasmas* **5**, 3986 (1998).
- [10] M.S. Smirnova, *Phys. Plasmas* **6**, 897 (1999).
- [11] K. Hanatani *et al.*, *Nucl. Fusion* **21**, 1067 (1981).
- [12] K. Hanatani *et al.*, *Nucl. Fusion* **25**, 259 (1985).
- [13] K. Hanatani and F.-P. Penningsfeld, *Nucl. Fusion* **32**, 1769 (1992).
- [14] T. Fujisawa *et al.*, *J. Plasma Fusion Res. SERIES* **1**, 84 (1998).